NOAA Technical Report NESS 73

Evaluation of a Balanced 300-mb Height Analysis as a Reference Level for Satellite-Derived Soundings

WASHINGTON, D.C.
JANUARY 1976

UNITED STATES DEPARTMENT OF COMMERCE
National Oceanic and Atmospheric Administration
National Environmental Satellite Service

NOAA TECHNICAL REPORTS

National Environmental Satellite Service Series

The National Environmental Satellite Service (NESS) is responsible for the establishment and operation of the environmental satellite systems of NOAA.

Publication of a report in NOAA Technical Report NESS series will not preclude later publication in an expanded or modified form in scientific journals. NESS series of NOAA Technical Reports is a continuation of, and retains the consecutive numbering sequence of, the former series, ESSA Technical Report National Environmental Satellite Center (NESC), and of the earlier series, Weather Bureau Meteorological Satellite Laboratory (MSL) Report. Reports 1 through 39 are listed in publication NESC 56 of this series.

Reports 1 through 50 in the series are available from the National Technical Information Service (NTIS), U.S. Department of Commerce, Sills Bldg., 5285 Port Royal Road, Springfield, Va. 22151, in paper copy or microfiche form. Order by accession number, when given, in parentheses. Beginning with 51, printed copies of the reports are available through the Superintendent of Documents, U.S. Government Printing Office, Washington, D.C. 20402; microfiche available from NTIS (use accession number when available). Prices given on request from the Superintendent of Documents or NTIS.

ESSA Technical Reports

NESC 40 Cloud Measurements Using Aircraft Time-Lapse Photography. Linwood F. Whitney, Jr., and E. Paul McClain, April 1967, 24 pp. (PB-174-728)

NESC 41 The SINAP Problem: Present Status and Future Prospects; Proceedings of a Conference Held at the National Environmental Satellite Center, Suitland, Maryland, January 18-20, 1967. E. Paul McClain, October 1967, 26 pp. (PB-176-570)

NESC 42 Operational Processing of Low Resolution Infrared (LRIR) Data From ESSA Satellites. Louis Rubin, February 1968, 37 pp. (PB-178-123)

NESC 43 Atlas of World Maps of Long-Wave Radiation and Albedo--for Seasons and Months Based on Measurements From TIROS IV and TIROS VII. J. S. Winston and V. Ray Taylor, September 1967, 32 pp. (PB-176-569)

NESC 44 Processing and Display Experiments Using Digitized ATS-1 Spin Scan Camera Data. M. B. Whitney, R. C. Doolittle, and B. Goddard, April 1968, 60 pp. (PB-178-424)

NESC 45 The Nature of Intermediate-Scale Cloud Spirals. Linwood F. Whitney, Jr., and Leroy D. Herman, May 1968, 69 pp. plus appendixes A and B. (AD-673-681)

NESC 46 Monthly and Seasonal Mean Global Charts of Brightness From ESSA 3 and ESSA 5 Digitized Pictures, February 1967-February 1968. V. Ray Taylor and Jay S. Winston, November 1968, 9 pp. plus 17 charts. (PB-180-717)

NESC 47 A Polynomial Representation of Carbon Dioxide and Water Vapor Transmission. William L. Smith, February 1969 (reprinted April 1971), 20 pp. (PB-183-296)

NESC 48 Statistical Estimation of the Atmosphere's Geopotential Height Distribution From Satellite Radiation Measurements. William L. Smith, February 1969, 29 pp. (PB-183-297)

NESC 49 Synoptic/Dynamic Diagnosis of a Developing Low-Level Cyclone and Its Satellite-Viewed Cloud Patterns. Harold J. Brodrick and E. Paul McClain, May 1969, 26 pp. (PB-184-612)

NESC 50 Estimating Maximum Wind Speed of Tropical Storms From High Resolution Infrared Data. L. F. Hubert, A. Timchalk, and S. Fritz, May 1969, 33 pp. (PB-184-611)

NESC 51 Application of Meteorological Satellite Data in Analysis and Forecasting. Ralph K. Anderson, Jerome P. Ashman, Fred Bittner, Golden R. Farr, Edward W. Ferguson, Vincent J. Oliver, Arthur H. Smith, James F. W. Purdom, and Rance W. Skidmore, March 1974 (reprint and revision of NESC 51, September 1969, and inclusion of Supplement, November 1971, and Supplement 2, March 1973), pp. 1--6C-18 plus references.

NESC 52 Data Reduction Processes for Spinning Flat-Plate Satellite-Borne Radiometers. Torrence H. MacDonald, July 1970, 37 pp. (COM-71-00132)

(Continued on inside back cover)

NOAA Technical Report NESS 73

Evaluation of a Balanced 300-mb Height Analysis as a Reference Level for Satellite-Derived Soundings

ALBERT THOMASELL, JR.

WASHINGTON, D.C.
JANUARY 1976

UNITED STATES DEPARTMENT OF COMMERCE
Rogers C.B. Morton, Secretary

National Oceanic and Atmospheric Administration
Robert M. White, Administrator

National Environmental Satellite Service
David S. Johnson, Director

CONTENTS

EVALUATION OF A BALANCED 300-MB HEIGHT ANALYSIS AS A REFERENCE LEVEL FOR SATELLITE-DERIVED SOUNDINGS

Albert Thomasell, Jr.
Meteorological Satellite Laboratory
National Environmental Satellite Service
NOAA, Washington, D.C.

ABSTRACT. A technique is developed and evaluated for using wind observations through application of the balance equation to improve the accuracy of objective height analysis in regions between height observations to provide reliable reference heights for satellite derived soundings. At upper levels (near 300 mb), numerous aircraft winds and satellite observed cloud vector winds are available for this purpose. In regions of moderate size, where the height analysis is determined primarily by winds and where the winds are deemed sufficiently dense and accurate, the technique produces interpolated height values with an estimated rms error of 30 m or less 80 to 85% of the time. Where these conditions are met it is concluded that the technique provides reliable reference heights.

1.0 INTRODUCTION

To obtain height profiles from satellite measured radiances, it is necessary to specify the height accurately at some arbitrary reference level (Smith, Woolf, and Fleming, 1972). These reference heights are usually obtained from an analysis at some specified constant pressure level: where observations are plentiful, there is no particular problem in obtaining a height analysis that is accurate within the noise limit of the data. In regions devoid of height observations, however, values must be interpolated to obtain a continuous analysis. In such regions, wind observations may be used in the interpolation process by the use of any one of several wind-height relationships.

It is the goal of this study to develop a technique that makes full use of wind observations for height interpolation in the analysis, and to evaluate the accuracy of such values with regard to their suitability as reference heights. The objective analysis technique developed and tested here uses the wind-height approximation embodied in the balance equation (e.g., Haltiner and Martin, 1957) to incorporate winds into the analysis of height. The technique was applied to data at the 300-mb level to exploit the normally abundant aircraft winds that are available at or near this level in otherwise data sparse regions over the oceans. The study was motivated primarily by the availability of these winds and the expected increase in high level satellite derived winds. Calculations performed on the polar stereographic grid provide an analysis for most of the Northern Hemisphere.

The basic technique used is the Conditional Relaxation Analysis Method (CRAM) (Thomasell and Welsh, 1963). Observations are used to define internal boundary point values on the grid, and then values interpolated for all nonboundary points require that the interpolated values satisfy the solution of a Poisson equation. The forcing function, the right-hand side of the Poisson equation, determines the shape of the resulting analysis at nonboundary points, and is calculated from whatever information is available for the problem at hand. The magnitude of the analyzed values is determined by peripheral boundary conditions and internal boundary values. The method thus permits nonlinear interpolation among data points accurate to the extent that the forcing function defines the true shape of the field.

The balance equation, written as a Poisson equation in height, has been used by Phillips (1959), Rosenthal (1960), and Endlich, Mancuso and Shigeishi (1971) to obtain height fields from wind fields, primarily in the tropics where direct height observations tend to be inadequate for accurate analysis. These investigators have shown that for an area comprising most of the United States, where data are dense and relatively consistent, the balance equation produces a height field that differs from a conventional height analysis by approximately 15 to 30 meters rms. Rosenthal (1960) showed that the largest differences tended to occur in low center where the balanced heights were too high. In general, however, there was quite good agreement between the shapes of the balanced and the conventional height analyses. Because of its ability to define shape well in regions where winds are plentiful, the balance equation is used in CRAM to calculate the required forcing function from winds for interpolation among height observations.

Here, the use of the balance equation differs from that used by the above investigators in two important aspects. First, the analysis area is much larger; it covers most of the Northern Hemisphere, rather than just the United States. Second, the concept of internal boundary points defined by the height observations is introduced to limit the size of regions requiring interpolation.

The balanced forcing function used for the height analysis is evaluated from a wind analysis. In the CRAM technique, wind is analyzed by components where the first guess is a geostrophic wind field with ageostrophic corrections obtained from a first-guess height field. Edited wind observations define internal boundary points and the Laplacian of the wind first guess comprises the forcing function. It is solely in the definition of the wind analysis that wind observations influence the subsequent height analysis.

For each case on which the analysis method was tested, two different CRAM height analyses were produced. One, the balanced-height analysis, was constructed entirely from the balanced forcing function and peripheral boundary conditions. This corresponds to the type of analysis produced by the above-mentioned investigators. The other, the final analysis, uses the same balanced forcing function, plus internal boundary values defined by observed heights. In both analyses, regions between boundary values contain interpolated heights that conform to the balance equation. These interpolated heights may ultimately serve as reference heights for satellite derived

soundings, so their accuracy is of prime concern. *A priori* one may assume this accuracy is a function of region size between boundary points, thus, the final analysis would be the better of the two. The basic reason for calculating the balanced-height analysis is to provide, where possible, direct measurements of the accuracy of balanced interpolated heights, using independent height observations, for a limited range of region size and wind quality. These measurements are then used to infer the accuracy in regions of the final analysis where no height observations are available.

2.0 THE ANALYSIS METHOD

2.1 Height Analysis

CRAM requires that the analysis of height Z at non-boundary points satisfy the Poisson equation

$$\nabla^2 Z = F, \tag{1}$$

where F is a forcing function that defines the shape of the Z field. To incorporate the balanced wind law into the analysis, we use the balanced forcing function for the polar stereographic grid (Deutscher Wetterdienst 1960) given by

$$\begin{aligned} F = {} & \frac{f\,\delta}{g}\,\zeta - \frac{\delta}{g}\,(\vec{V} \times \nabla f) \cdot \vec{k} - \frac{2}{g} m^2 J(V,U) \\ & - \frac{1}{g}\,\nabla K \cdot \nabla m^2 - \frac{K}{g}\,\nabla^2 m^2 \\ & - \frac{1}{g}\left(V \frac{\partial U}{\partial y} - U \frac{\partial V}{\partial y}\right) \frac{\partial m^2}{\partial x} \\ & - \frac{1}{g}\left(U \frac{\partial V}{\partial x} - V \frac{\partial U}{\partial x}\right) \frac{\partial m^2}{\partial y}, \end{aligned} \tag{2}$$

where δ is the reference grid increment (381 km), m is the local map factor, f is the coriolis parameter, and g is the acceleration of gravity. The vector $\vec{V}$ and its components U and V are scaled winds (Stackpole 1969) and are the true winds divided by the local map factor. The other symbols of (2) are defined by

$$\zeta \equiv \frac{\partial V}{\partial x} - \frac{\partial U}{\partial y},$$

$$J(V,U) \equiv \frac{\partial V}{\partial x}\frac{\partial U}{\partial y} - \frac{\partial V}{\partial y}\frac{\partial U}{\partial x},$$

$$K \equiv \frac{U^2 + V^2}{2}.$$

Equation 2 shows that F is a function only of the wind field and latitude.

Equation 1 is here solved by the implicit alternating-direction relaxation method, described by Mancuso (1967), which iterates on complete rows and columns rather than point by point. The method is applied with normal derivative boundary conditions obtained from the NMC operational 300-mb height analysis.

For the final analysis, those observations of height which define internal boundary points are not permitted to change value during the relaxation solution of (1). Since observations normally do not coincide with gridpoints, their information must in some way be translated to gridpoints for subsequent use in the analysis technique. In this study, a value from the first-guess field is interpolated at the location of the observation and the difference between the observation and the interpolated first guess value is added to the first guess at the nearest gridpoint. If more than one observation affects a gridpoint, an average difference is used to define the internal boundary value. The relaxation procedure forces the remaining gridpoints to assume values dictated by the forcing function, the internal boundary values, and the peripheral boundary conditions. To eliminate small scale irregularities, a mild smoothing filter is applied to the analysis as a final step.

2.2 Wind Analysis

In wind analysis, each component is analyzed separately. A first-guess field is obtained for each wind component by calculating a geostrophic wind field from a moderately smoothed version of the NMC height analysis. Smoothing was found necessary to suppress spurious, large geostrophic winds at low latitudes. Smoothing also has the deleterious effect of attenuating small scale features and of reducing the height gradient, and, hence, the geostrophic wind speed throughout the analysis area. The geostrophic wind field is modified to include ageostrophic corrections as outlined by Arnason, *et al.* (1962).

Each wind component is analyzed by the CRAM method in which the forcing function is defined as the Laplacian of the modified first-guess field. All available edited wind observations are used to define internal boundary values, and the Poisson equation is solved by relaxation with fixed peripheral and internal boundary values. As a final step, the wind analysis is smoothed lightly with a filter (Thomasell *et al.* 1966) to remove small scale irregularities.

For one series of tests, the analyzed winds were used in unmodified form to calculate F in equation (1). These winds are later referred to as divergent winds. In another series, the winds were made non-divergent by Endlich's (1967) method of altering wind fields.

2.3 Data Error Checking

Because the NMC analysis, itself the product of a comprehensive error checking procedure, is readily available, it is used as the basis for detecting errors in both the height and wind observations used in this study.

Height error checking is simple. If a height observation differs from the NMC analysis by more than 100 meters, it is discarded. With this discard limit, surviving heights agree with the NMC analysis within 30 meters rms.

Wind vectors are checked by comparing them with geostrophic wind vectors interpolated from the NMC analysis at the locations of the wind observations. The error detection method is essentially the same as that devised by Endlich *et al.* (1971). Let $\vec{V}_L$ represent the larger of the two wind vectors and $\vec{V}_S$, the smaller. Then the ratio of the dot product of the two vectors to the square of the larger wind speed,

$$R = \frac{\vec{V}_S \cdot \vec{V}_L}{|\vec{V}_L|^2} = \frac{|\vec{V}_S|}{|\vec{V}_L|} \text{ Cos } \Theta,$$

provides a useful decision index for error checking. The angle between the two winds is given by θ. The ratio R expresses the projection of the smaller vector on the larger vector as a percentage of the larger wind speed. The maximum value of R is +1, which results when $\vec{V}_S$ and $\vec{V}_L$ are identical. When the vectors are equal in magnitude but opposite in direction, (θ=180°), a minimum value R=-1 is obtained. Orthogonal vectors produce R=0. An observed wind vector is discarded if

$$R < R_{min},$$

where R_{min} is a parameter that controls the maximum angular departure θ and the maximum difference in wind speed for a given $\vec{V}_L$. In practice, this method of wind error checking and, in particular, the value $R_{min} = 0.3$ appears to be satisfactory.

2.4 Aircraft Wind Editing

The observations used in the wind analyses are synoptic rawinsonde and bogus winds at 300 mb, and aircraft winds that are usually both asynoptic and off-level. The raw aircraft winds generally present a chaotic picture and require some editing and modification.

First, the aircraft winds are screened and all observations outside the altitude interval 25,000 ft to 38,000 ft and the time interval $\pm$ 6 hours from map time are discarded. Then, the aircraft winds are made quasi-synoptic by advecting them in a smooth steering flow--forward for early data and backward for late data--for a distance proportional to the steering flow and the age of the report. Large-scale steering flows have been described by Thomasell and Welsh (1968) and Nagle and Hayden (1971). The steering flow used here was obtained by smoothing the first guess height field to eliminate features of synoptic scale and smaller.

After the aircraft winds are edited and modified, they are subjected to the wind error checking method described in the previous section.

Figure 1a, for January 18, 1970 at 0000 GMT, shows a typical set of unedited winds available for analysis at the 300-mb level. The larger barbs represent rawinsonde and bogus winds; the smaller barbs, found only over ocean regions, are aircraft winds. Figure 1b shows the same set of winds after

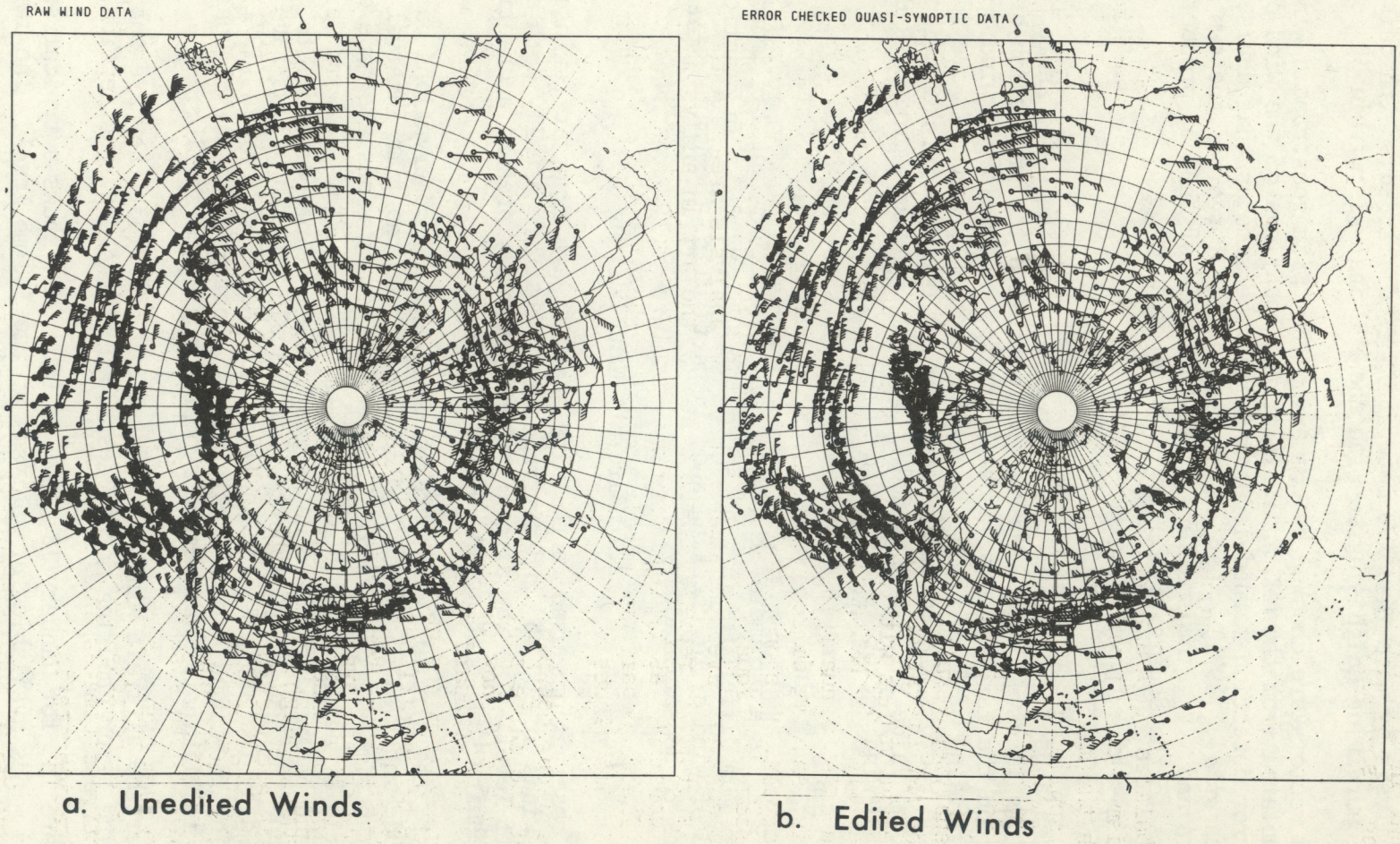

Figure 1.--Aircraft winds near 300 mb, 300-mb rawins, and bogus winds for 18 January 1970, 00Z.

editing. A careful inspection of these figures reveals a significant improvement in the spatial coherence of the winds after editing and error checking, especially among the aircraft winds.

3.0 EXPERIMENTAL RESULTS

3.1 Details of the Experiment

The balance equation, written as a Poisson equation in height, provides a mechanism for incorporating winds into the analysis of pressure height through the medium of the CRAM analysis technique. Test results of the method applied to 300-mb data are presented and evaluated here. The 300-mb level was chosen because of the abundance of aircraft winds in otherwise data sparse regions.

The analyses resulting from these tests were evaluated by comparing them with the NMC operational 300-mb height analysis, and with observed radiosone height values within selected subsections of the analysis area. Comparisons with the NMC analysis presented in graphical and numerical form for one case, January 18, 1970, at 0000 GMT show the NMC analysis, the CRAM analysis, and the difference field representing the CRAM analysis minus the NMC analysis. The numerical comparisons shown in tabular form give the mean, root-mean-square, and standard deviation of the difference between the two analyses averaged over the entire analysis area. Although the NMC analysis probably represents the state-of-the-art in analysis, it should not be construed as representing the absolute truth throughout the analysis area. These comparisons merely point out the differences between the two analysis techniques.

Comparisons between CRAM analyses and observed heights are calculated for each of the three subareas shown in figure 2. The results presented in tables 1 and 2 show the number of observations and the mean, root-mean-square, and standard deviation of the difference parameter (defined as the CRAM analysis minus observed height). The central area statistics give a measure of overall performance and show whatever large scale biases exist. The United States and Europe statistics are representative of analysis performance on the synoptic scale; both represent regions of dense observations of height and wind. For the balanced height analyses, (table 1), in which no observed heights were used, the statistics give a true measure of the analysis accuracy within the noise limitations of the data and the grid interpolation process. For the final analysis, (table 2), the statistics merely indicate how closely the analysis technique forced the analysis to fit the data; in this sense, they give a measure of the data noise. It is of primary importance here to evaluate the accuracy of the interpolated height analysis in regions between height observations where winds are available. Subjective estimates of this accuracy were inferred from the balanced-height verification statistics.

Two series of analyses were calculated for each test case. A series consisted of constructing a wind analysis, evaluating a balanced forcing

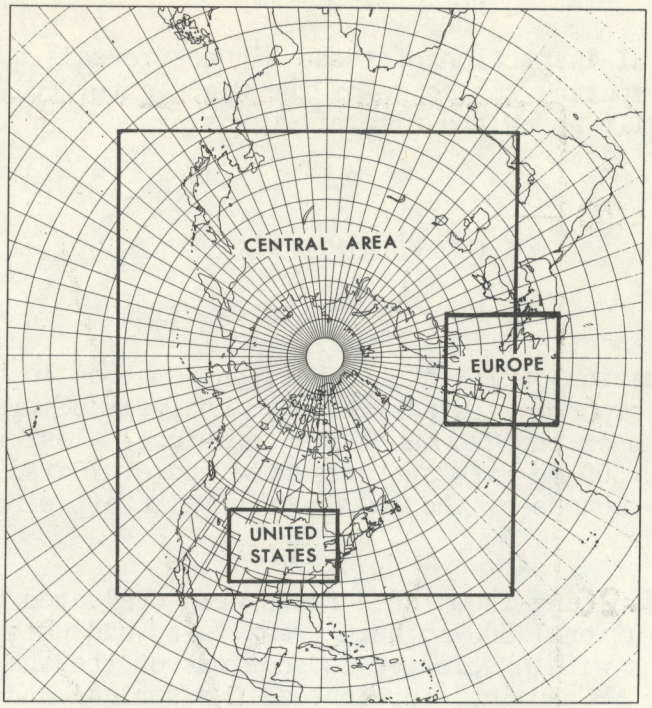

Figure 2.--Analysis evaluation areas.

function, and then producing a balanced height analysis and a final height analysis. Data for each test case consisted of error-checked rawinsonde observations of 300-mb heights and winds, bogus heights and winds, and edited aircraft winds. The NMC 300-mb analysis was used for the first-guess height field. For the first series, the wind analysis used for evaluating the balanced forcing function was made nondivergent. Endlich's method (1967) for altering the properties of wind fields was used for this purpose. The use of a nondivergent wind field resulted in a marked negative bias in the balanced height analysis in comparison with both the NMC analysis and the observed heights. A second series of analyses was subsequently calculated in which the original, unaltered, divergent wind field was used for calculating the balanced forcing function. This shift to a divergent wind analysis in most cases effected a marked decrease in the negative bias of the balanced height analysis.

3.2 Evaluation of the Balanced Height Analyses With Observed Heights

The experimental results of comparing the balanced height analyses with observed heights for three cases are summarized in table 1. Some of the more important points to be drawn from table 1 are illustrated in figure 3.

Figure 3 shows that, in the central verification area, a region that encompasses most of the variability in the height field in the Northern Hemisphere, all the maps exhibit a negative mean error, i.e., the balanced height analysis in this area tends toward lower than observed heights.

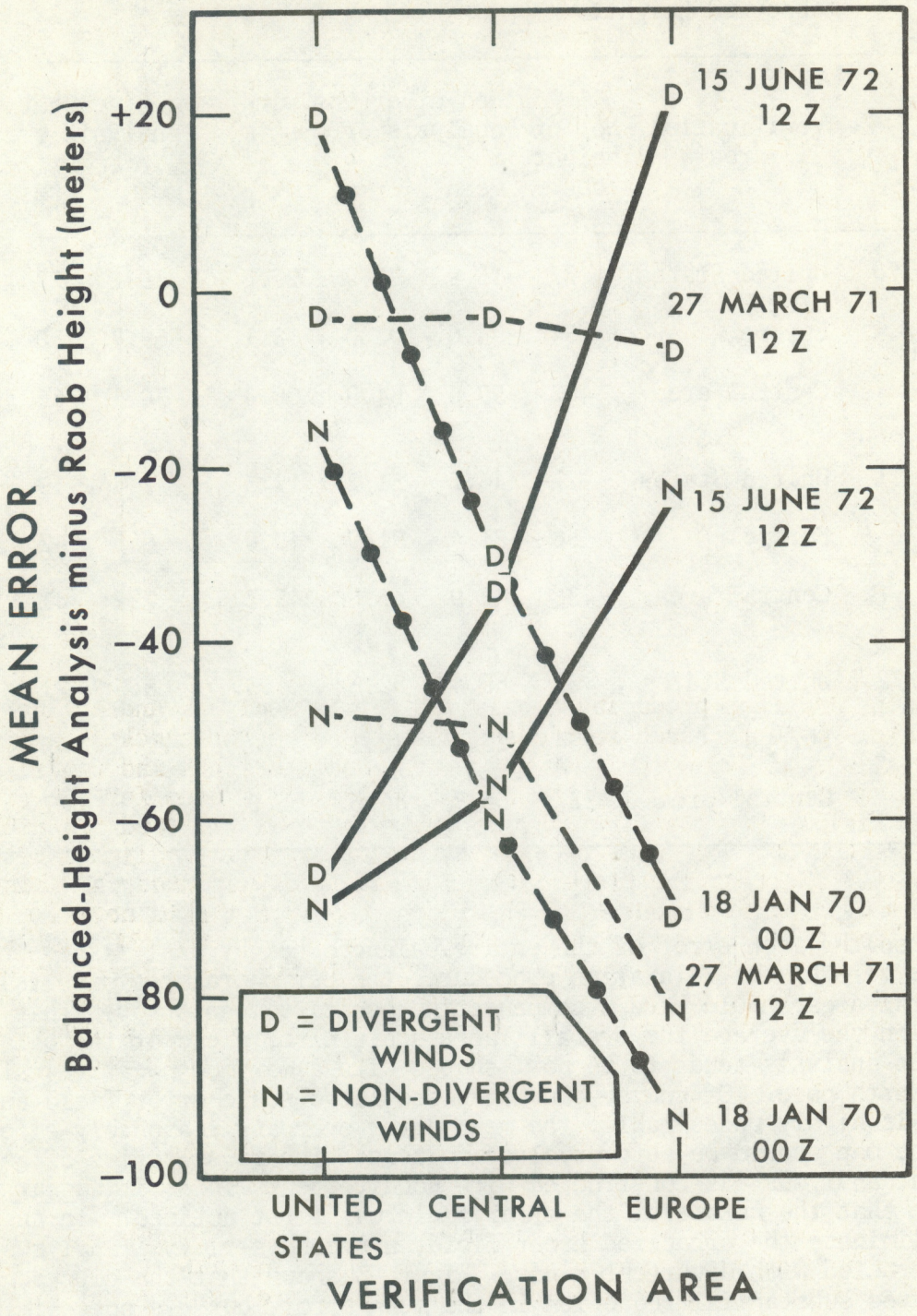

Figure 3.--Mean errors of the balanced height analyses compared with observed heights.

Table 1.--Verification statistics for balanced-height analysis minus observed height.

Case	Verification area	No. of height obs.	Non-divergent wind analysis errors (m)			Divergent wind analysis errors (m)		
			mean	rms	σ_E	mean	rms	σ_E
1/18/70	United States	27	-15.9	25.9	20.5	19.1	27.4	19.6
00Z	Europe	54	-94.6	102.0	38.1	-69.7	80.4	40.1
	Central area	402	-59.6	84.9	60.4	-30.1	66.7	59.5
3/27/71	United States	27	-48.2	51.2	17.3	- 2.4	19.8	19.7
12Z	Europe	56	-81.4	91.0	40.8	- 6.3	42.4	41.9
	Central area	425	-48.9	66.6	45.2	- 2.5	41.4	41.3
6/15/72	United States	22	-69.4	82.3	44.3	-68.5	81.9	44.7
12Z	Europe	34	-23.7	42.1	34.8	22.5	40.8	34.1
	Central area	257	-56.7	86.3	65.0	-33.6	77.0	69.3

Because the mean error of the entire balanced height analysis is forced to be zero by the relaxation procedure, the peripheral region outside the central area should have a compensating positive mean error. This implies that on the average the overall large scale error field of the balanced height analysis tends to be bowl-shaped with a maximum negative value near the north pole. Of course, an organized large-scale error field such as this is highly undesirable; the mean error over any reasonably-sized area of the map should be zero or close to zero. The first series of balanced height analyses was constructed with nondivergent winds; it was at this point that the nature of the error field was first noticed. In an attempt to eliminate the organized error field, a second series of analyses was constructed with divergent winds. Figure 3 shows that the divergent winds effected substantial reduction in the mean error, but did not eliminate the negative bias.

The divergent case for 27 March 1971 shows remarkable improvement with near-zero mean error; however, the other two cases, for 15 June 1972 and 18 January 1970, although improved, still show an unacceptable mean error

Table 2.--Verification statistics for final analysis minus observed height.

Case	Verification area	No. of height obs.	Non-divergent wind analysis errors (m) mean	rms	σ_N	Divergent wind analysis errors (m) mean	rms	σ_N
1/18/70	United States	27	-0.3	15.4	15.4	-0.2	15.4	15.4
00Z	Europe	54	0.5	22.9	22.9	0.4	23.0	22.9
	Central area	402	-0.1	24.1	24.1	-0.1	24.1	24.1
3/27/71	United States	27	-1.8	11.7	11.6	-1.8	11.7	11.6
12Z	Europe	56	4.4	29.3	28.9	4.4	29.3	28.9
	Central area	425	1.0	22.2	22.2	1.0	22.2	22.2
6/15/72	United States	22	-1.5	22.5	22.5	-1.5	22.6	22.6
12Z	Europe	34	5.2	21.9	21.3	5.2	22.0	21.4
	Central area	257	0.4	23.8	23.8	0.4	23.8	23.8

of approximately -30 meters. The reason for this large scale negative bias is believed to be related to incomplete compensation for the cyclonic curvature of the polar vortex with respect to the balanced wind law implicit in the analysis technique. This results in a small but cumulative error directed toward the North Pole.

In Figure 3, the small United States and Europe verification areas show large fluctuations in mean error compared to the mean error of the central area. This implies that the mean error in small regions is strongly dependent upon synoptic scale phenomena. An examination of the maps presented later will show that mean errors with magnitudes toward the positive end of the mean error scale are generally associated with cyclonic curvature and large negative errors with anticyclonic curvature. Thus the amplitude of synoptic scales is systematically attenuated in the balanced height analysis. Further, the relative error associated with synoptic scale features is essentially independent of the divergent character of the wind field. This is indicated in table 1 by the very small differences in the standard deviation for a given verification area between a divergent and a non-divergent wind. The probable cause for most of the systematic loss of

amplitude in synoptic scale features is excessive smoothing throughout the analysis process.

The overall error field of a balanced height analysis thus appears to have two primary components; one, a large-scale, more-or-less bowl-shaped field, and the other, a highly variable field correlated with synoptic scale curvature superimposed on the first.

In terms of the root-mean-square error (rms) shown in table 1, the balanced height analyses vary greatly in accuracy from one area to another within a given map and also from one map to another. The central area, with the exception of the divergent case for 27 March 1971, has a relatively large rms error. The rms error in the United States and Europe alternate between relatively good values and quite poor values. This high variability in accuracy, coupled with the persistent negative bias described above, clearly indicates that on a hemispheric scale the balanced height analysis, without some modification, does not provide a consistent, reasonably accurate representation of the 300-mb height field.

The standard deviation (σ) of the balanced height analysis, is a measure of the accuracy of the shape of the analysis field, since it represents the error with the bias removed. For the three cases given in table 1, this accuracy tends strongly to be inversely proportional to the size of the verification area. For a region the size of the central area, the error is usually unacceptably large. This dependence of analysis accuracy on region size is used extensively in the next evaluation.

3.3 Evaluation of the Final Analysis With Observed Heights

Evaluation of the final analysis is a two-step process. In the first step, a simple comparison is made between the final analysis and the height observations used in its construction. In the second step, an attempt is made to estimate the error of interpolated height values in regions between observed heights. For this purpose, extensive use is made of the results obtained in evaluating the balanced height analyses.

Table 2 gives the results of the first step for three cases in terms of the mean, the root-mean-square, and the standard deviation of the measured difference between the final analysis and height observations within each of the three verification areas. The standard deviations in this table are a measure of how closely the observations were forced to fit the final analysis. (It should be noted that these standard deviations are almost equivalently the rms values since the mean differences are quite small.) In the dense data areas, Europe and the United States, it is assumed that the final analysis is error-free insofar as the scales resolved on the analysis grid are concerned. Thus the standard deviation for these areas is a measure of the data noise level. This quantity, denoted by σ_N, is used in the subsequent evaluation.

In the final analysis, the regions of interpolated heights are, in reality, balanced height analyses with fixed boundary values defined by height observations. Region size is highly variable and depends upon the

spatial distribution of the observations. In the smaller regions, the boundary values, for all practical purposes, eliminate bias in the interpolated heights. This fact makes it possible to estimate the error of the interpolated heights from the balanced height analysis results described in the previous section through the concept of equivalent regions.

An equivalent region in the final analysis is a region devoid of height observations in which the interpolated heights have zero bias. In addition it must approximately resemble one of the verification areas for which balanced height measurements are available (the United States or Europe), with respect to region size and quality and distribution of winds contained within the region.

Because most of the factors that determine the interpolated analysis in an equivalent region must be identical to those that determine the balanced height analysis in the United States or Europe areas, the two types of analyses should have similar errors. The standard deviation statistic for balanced height analyses, as given in table 1, meets the requirement for zero bias and provides the desired estimate of the interpolated analysis error in the equivalent regions of the final analysis. This statistic, called the balanced height error, is given the symbol σ_E, where the subscript E refers to the fact that the height data used for evaluating the statistic contain random errors or noise.

A third statistic, the true error σ_T, which is useful for the evaluation of interpolation error in the final analysis may be calculated from data noise σ_N and balanced height error σ_E. The true error σ_T represents the analysis error in an interpolation region as measured by error-free height data. The true error has the property of being independent of height data noise; its variations within a fixed region reflect variations in the accuracy and distribution of wind observations and variations due to limitations of the balanced wind law in coping with circulation patterns with marked curvature. The true error is calculated by

$$\sigma_T^2 = \sigma_E^2 - \sigma_N^2,$$

under the assumption that the true analysis error at a data point is uncorrelated with the data noise there. A useful interpretation of σ_T is that, within an equivalent region, it represents the difference between a balanced height analysis with zero bias and an analysis (assumed perfect) constructed from a dense network of height observations. In this sense, σ_T is directly comparable to the verification statistic used by Phillips (1959), Rosenthal (1960), and Endlich *et al.* (1971) for evaluating their balanced height analyses.

Tables 1 and 2 give values of σ_N and σ_E for three separate cases for the Europe and the United States verification areas. It is evident from these tables that both σ_N and σ_E undergo significant changes from case to case and from one area to another. To help describe this variability with greater certainty, values of σ_N, σ_E, and σ_T were calculated for 28 cases. Their frequency distributions, for 5-meter intervals, are given in table 3 for the United States and Europe areas. Table 3 shows that the distributions for

Table 3.--Frequency distribution of the verification parameters σ_E, σ_T, and σ_N obtained from 28 cases

Value of σ parameter (5-m intervals)	Frequency of occurrence (%)					
	United States			Europe		
	σ_E	σ_T	σ_N	σ_E	σ_T	σ_N
0 - 4.9	0.0	0.0	0.0	0.0	0.0	0.0
5.0 - 9.9	0.0	7.1	0.0	0.0	0.0	0.0
10.0 - 14.9	3.6	10.7	46.4	0.0	3.6	0.0
15.0 - 19.9	10.7	39.3	42.9	0.0	17.9	46.4
20.0 - 24.9	32.1	10.7	10.7	7.1	32.1	5.0
25.0 - 29.9	28.6	17.9	0.0	17.9	17.9	3.6
30.0 - 34.9	10.7	7.1	0.0	42.9	10.7	0.0
35.0 - 39.9	7.1	3.6	0.0	3.6	14.3	0.0
40.0 - 44.9	3.6	0.0	0.0	25.0	0	0.0
45.0 - 49.9	3.6	3.6	0.0	3.6	3.6	0.0

Table 4.--Mean and standard deviation (σ) of the verification parameters σ_E, σ_T, and σ_N obtained from 28 cases

Verification parameters	Verification area			
	United States		Europe	
	Mean	σ	Mean	σ
	(m)	(m)	(m)	(m)
σ_E	26.9	8.0	34.0	6.4
σ_T	21.3	8.6	26.7	7.4
σ_N	15.8	3.2	20.5	2.4

σ_E and σ_T are not gaussian, but, rather, are skewed with peak frequencies tending toward the lower values. The means and standard deviations of the three verification parameters σ_E, σ_T, and σ_N for the United States and Europe verification areas are given in table 4.

Data noise, σ_N, is seen in tables 3 and 4 to be greater in Europe than in the United States; however, in both areas the values of noise are restricted to a relatively narrow range. For the United States area, about 90% of the noise values lie in the range 10 to 20 meters; in Europe, over 95% of the noise values are in the range 15 to 25 meters. The mean noise level in the United States area is 15.8 meters and in Europe is 20.5 meters. The greater noise level in the Europe area may be attributed to the use there of a relatively large number of different types of radiosonde instruments.

Whether σ_E or σ_T is chosen as a measure of interpolation error in equivalent regions of the final analysis, it is apparent from the wide distribution of these parameters in tables 3 and 4 that no single value is representative of the interpolation error. The error may be meaningfully expressed only in terms of a probability statement. Toward this end, estimated probability distribution functions constructed from the data in table 3 are presented in figure 4. Each function gives the probability that σ, now treated as a continuous random variable, will be equal to or less than some prescribed value σ_{MAX}. Functions are given for σ_T and σ_E for the Europe and United States verification areas. By coincidence, the functions for σ_E in the United States and for σ_T in Europe were so nearly alike that they are given as a single curve in figure 4.

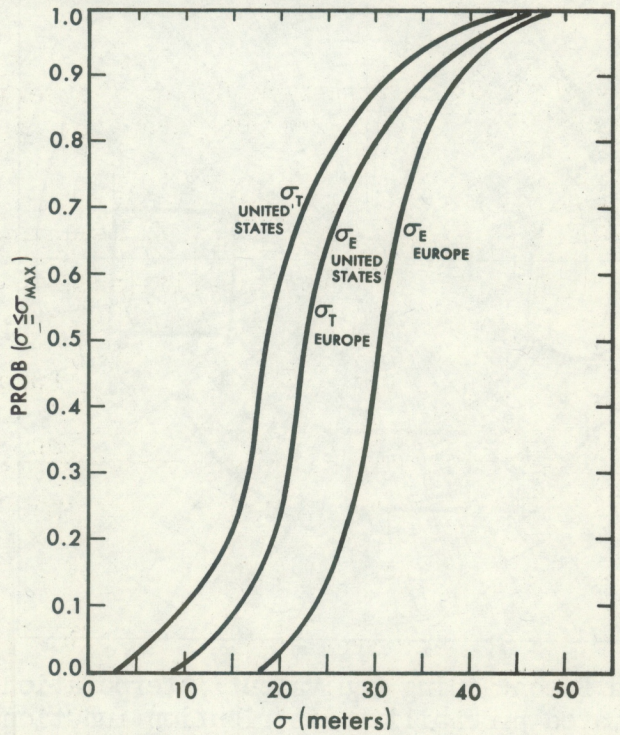

Figure 4.--Estimated probability distribution functions for σ_T and σ_E for Europe and the United States.

The σ_T function for the Europe area for most probability levels is roughly only 5 meters larger than that for the United States and one half the difference between the corresponding σ_E functions. Thus, σ_T is somewhat more independent of area than σ_E. The slightly lower values of σ_T for the United States area, compared with those for Europe, may be mainly ascribed to the smaller size of the United States area, although some of the difference may be due to slightly more accurate or consistent winds in the United States.

The large range of values associated with σ_E and σ_T within a given verification area is directly related to two factors, wind quality and intensity of curvature in the height field. The high values of σ are associated with wind sets of inferior quality, marked curvature, or both, and the low values with unusually good wind sets or smooth height contours with little curvature.

The practical determination of equivalent regions is made difficult by the lack of reliable measures of wind accuracy. For this study they were established by subjective comparisons of wind sets. The equivalent regions, of course, may occur at any locations throughout the analysis area where the required conditions are met. On the other hand, no estimate of the interpolation error can be made for the final analysis where the region is too large or where the wind data are insufficient.

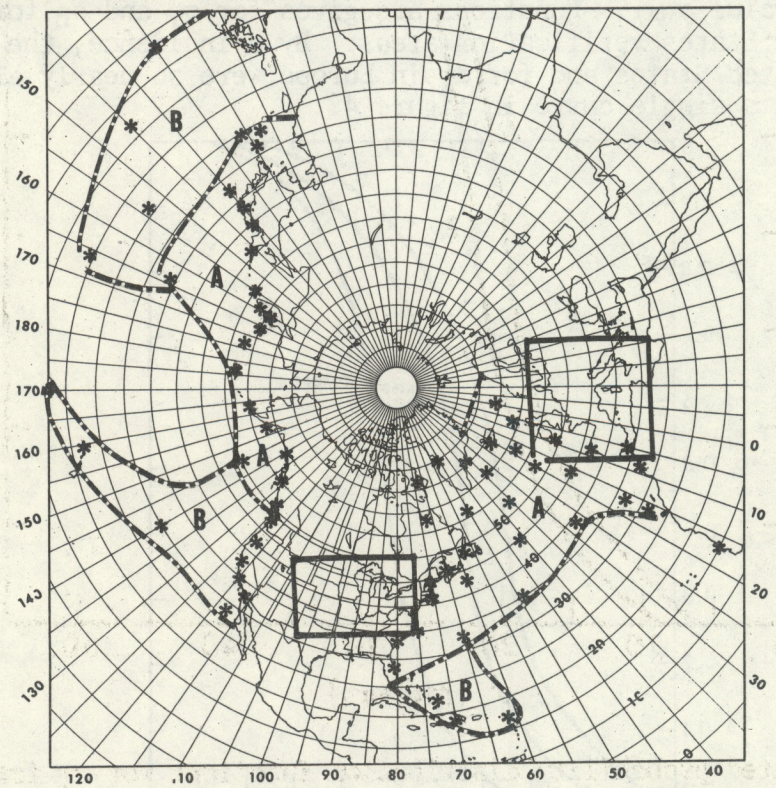

Figure 5.--Zones A and B containing equivalent interpolation regions for which estimated probability distribution functions σ_T are given in figure 6. Asterisks indicate the locations of radiosonde stations from which height observations are normally available.

Figure 5 shows two different zones within which it was deemed possible to estimate interpolation error; within each of these are a number of individual interpolation regions that, subjectively, are judged to be approximately homogeneous. The asterisks in figure 5 indicate the locations of rawinsonde stations where height observations (used as internal boundary points) are normally available. The spaces between the height observations are the interpolation regions for which estimates of analysis error are desired. In the oceanic regions excluded from zones A and B in figure 5, in particular the large mid-Pacific area, there normally are not enough wind observations to qualify these areas as equivalent regions.

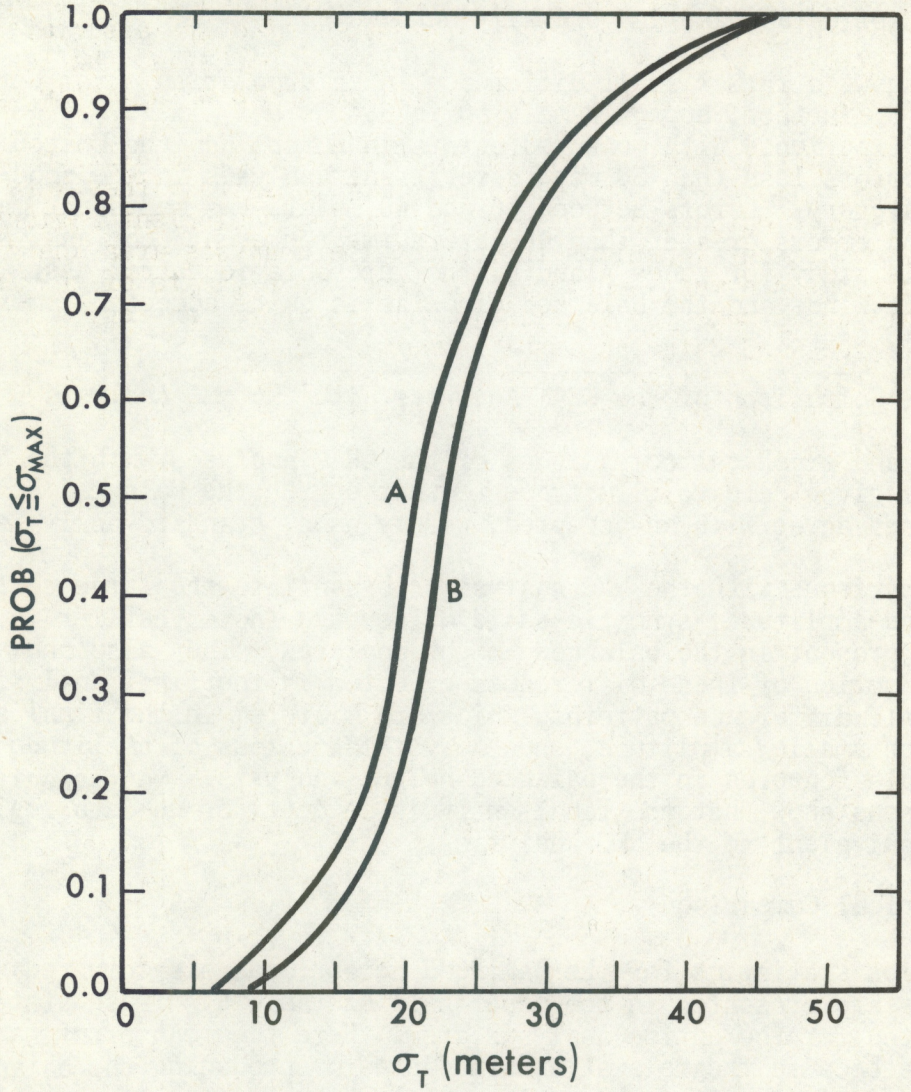

Figure 6.--Estimated probability distribution functions for σ_T for the interpolation regions in zones A and B shown in figure 5.

Figure 6 shows estimated probability distribution functions for the parameter σ_T for zones A and B. The interpolation regions in zone B were judged to be equivalent to the Europe area; the B curve in figure 6 is identical to the Europe area σ_T curve in figure 4. The interpolation regions in zone A, based on a trade-off between region size and wind quality, were judged to be slightly inferior to the United States area, primarily because of the consistently high wind quality available in the United States area. For lack of numerical measures of quality, the zone A curve in figure 6 was arbitrarily placed midway between the United States area and the Europe area σ_T curves shown in figure 4. No error functions for σ_E are given in figure 4 because this parameter is data-noise dependent, and the geographical distribution of data noise is generally unknown.

Figure 6 shows a rather small difference in interpolation error between zones A and B; further, approximately 80 to 85% of the time σ_T is less than 30 meters. Experience with measured errors in Europe and the United States shows that errors less than 30 meters represent analyses in the good-to-excellent category. Errors between 30 and 40 meters rms represent marginal analyses, and errors greater than 40 meters rms represent poor analyses. Thus, in this study for zones A and B, the interpolation error associated with aircraft winds and the balanced wind law is quite acceptable most of the time.

3.4 Comparison of the CRAM Analyses With the NMC Analysis

Numerical and graphical comparisons of the CRAM analyses with the NMC analysis are given here to illustrate to what degree the balanced height and final analyses agree with an accepted, widely used, standard analysis.

These comparisons with the NMC analysis substantiate the large scale bias and the large-amplitude, synoptic-scale difference (noted earlier in table 1) that are present in the balanced height analyses. They also show the dramatic reduction of these differences effected by the final analysis. The synoptic scale difference patterns, which are mirrored in the final analysis, but with much smaller amplitude, show a systematic loss of amplitude of synoptic scale features in the balanced height analysis. Most significantly, the comparisons show that the final analysis, except for no-data regions, is virtually equivalent to the NMC analysis.

3.4.1 Numerical Comparison

Verification statistics for the balanced height analysis compared with the NMC analysis are presented in the upper half of table 5. These statistics are calculated for the entire analysis area. Here the mean error has little significance because the relaxation procedure for producing the balanced height analysis forces it to be small. With the exception of the relatively good divergent wind analysis case for 27 March 1971, the rms differences are seen to be quite large. In contrast, the final analysis comparisons with the NMC analysis, shown in the lower half of Table 5, indicate markedly smaller rms differences, map for map.

Table 5.--Hemispheric comparison of balanced-height and final analyses with the NMC analysis

Analysis comparison	Case	Non-divergent wind analysis errors (meters)			Divergent wind analysis errors (meters)		
		Mean	rms	σ	Mean	rms	σ
Balanced-height analysis minus NMC analysis	18 Jan 1970 00Z	-3.3	60.8	60.7	-1.8	57.1	57.0
	27 Mar 1971 12Z	-3.0	57.0	56.9	-1.1	41.8	41.8
	15 Jun 1972 12Z	-2.7	77.8	77.8	-1.5	81.8	81.8
Final height analysis minus NMC analysis	18 Jan 1970 00Z	7.6	31.5	30.6	0.1	28.5	28.5
	27 Mar 1971 12Z	12.5	33.6	31.1	6.2	32.1	31.5
	15 Jun 1972 12Z	7.5	45.6	44.9	2.0	49.0	49.0

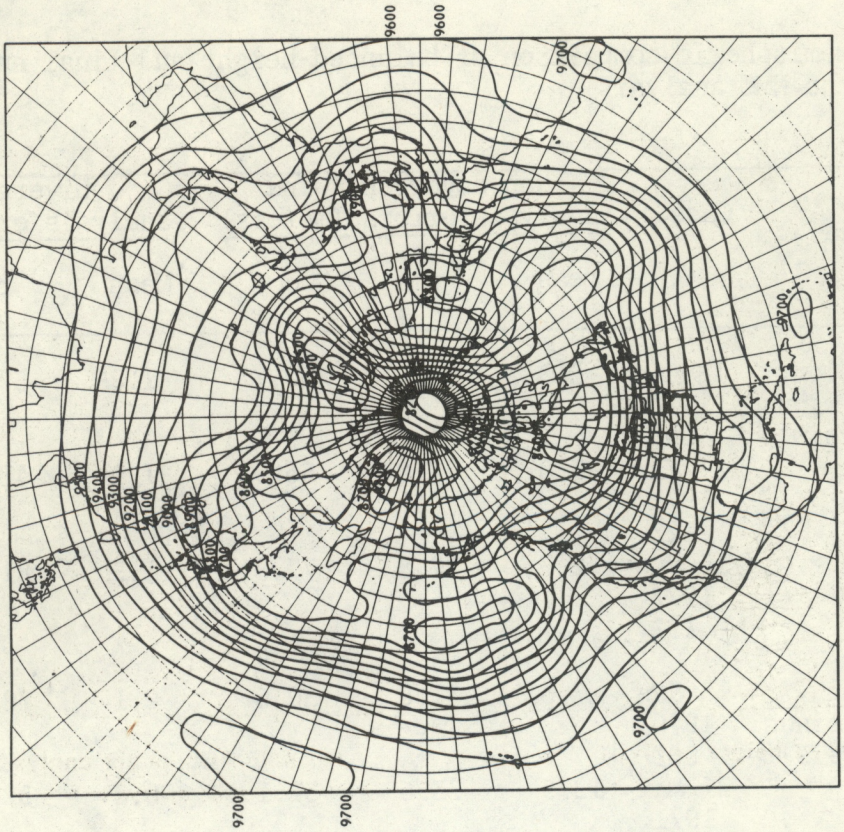

Figure 7.--The NMC 300-mb analysis for 18 January 1970, 0000 GMT.

3.4.2 Graphical comparison

The NMC 300-mb analysis for 18 January 1970, a typical case, is shown in figure 7. The measured winds available for this case are plotted in figure 1a (section 2.4) and the corresponding edited winds, in figure 1b. A conspicuous gap in wind coverage is apparent in the Pacific south of Alaska. This gap coincides with an elongated trough and ridge system in the NMC analysis. The balanced height analysis with divergent winds (fig. 8a) completely fails to define this system, presumably because of the lack of data. Outwardly, figure 8a resembles the NMC analysis, but suffers from an overall loss of smaller scale detail.

The difference field between the divergent-wind, balanced-height analysis and the NMC analysis is shown in figure 8b. Here, a pronounced negative bias is apparent, especially over Europe, Africa, Asia, and the western Pacific. Synoptic scale patterns in the difference field with values in the range $\pm$ 200 meters are associated with a systematic and substantial erosion of wave amplitude in figure 8a. Figures 9a and 9b show similar results for the nondivergent wind case, but display a larger overall negative bias in mid and upper latitudes.

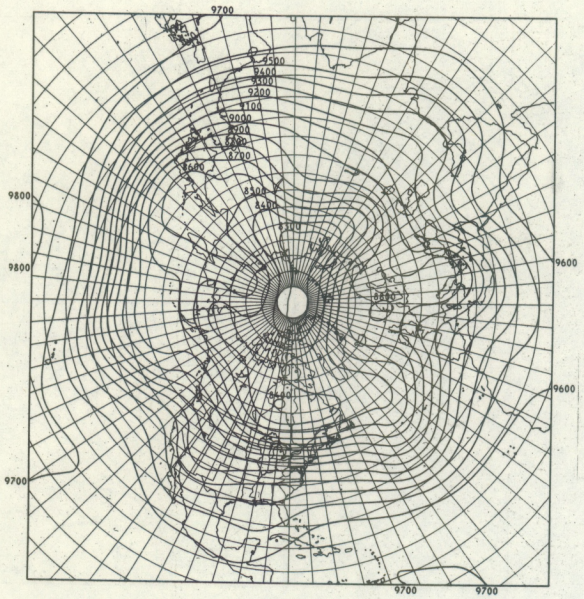

a. Balanced height analysis

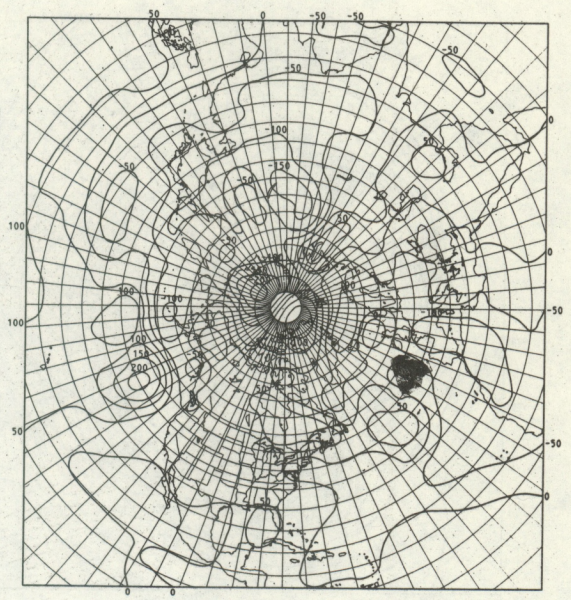

b. Balanced height analysis minus the NMC analysis

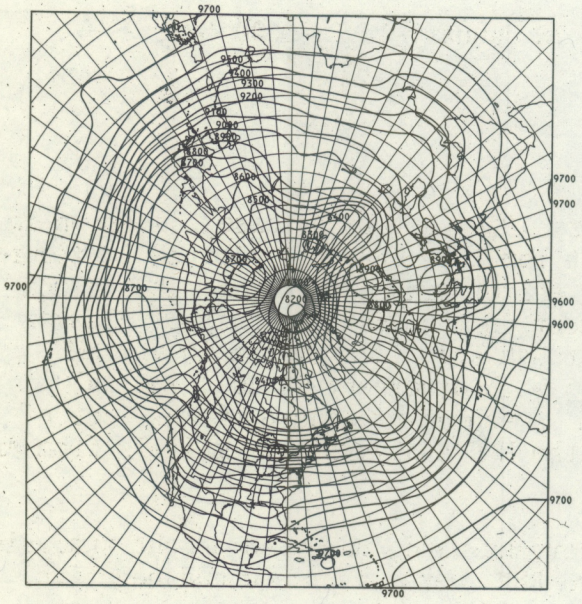

c. Final analysis

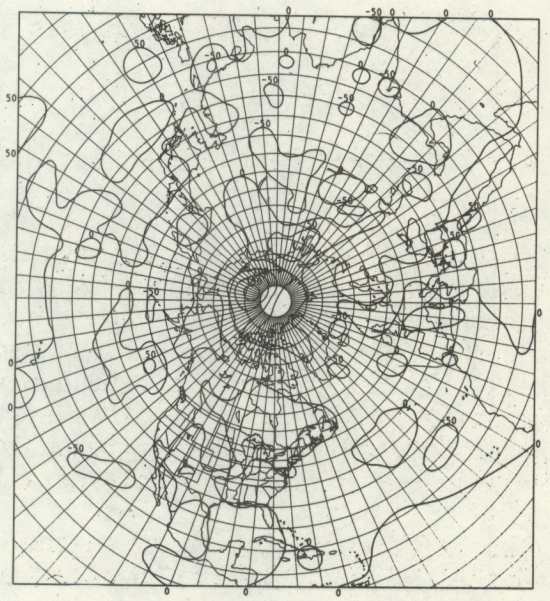

d. Final analysis minus the NMC analysis

Figure 8.--CRAM analyses and their comparisons with the NMC analysis for 18 January 1970, 0000 GMT. Divergent wind case.

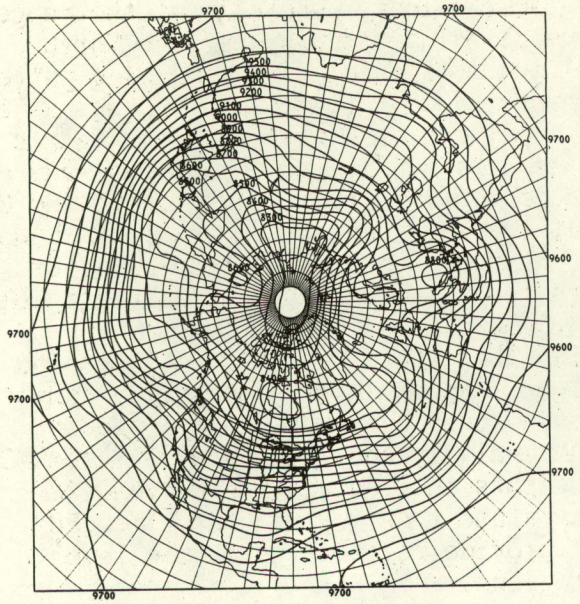

a. Balanced height analysis

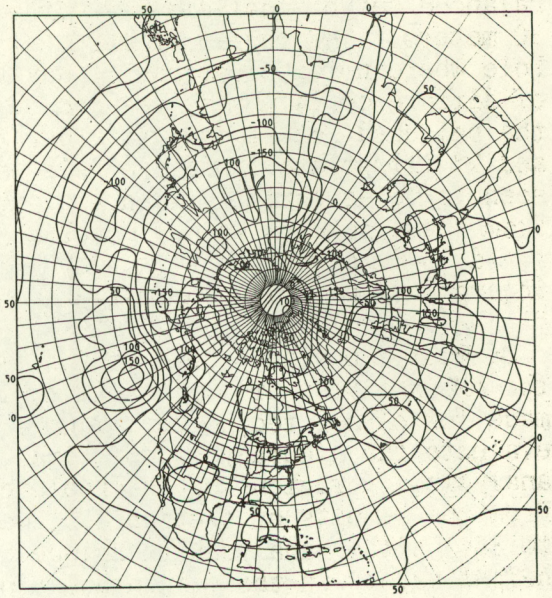

b. Balanced height analysis minus the NMC analysis

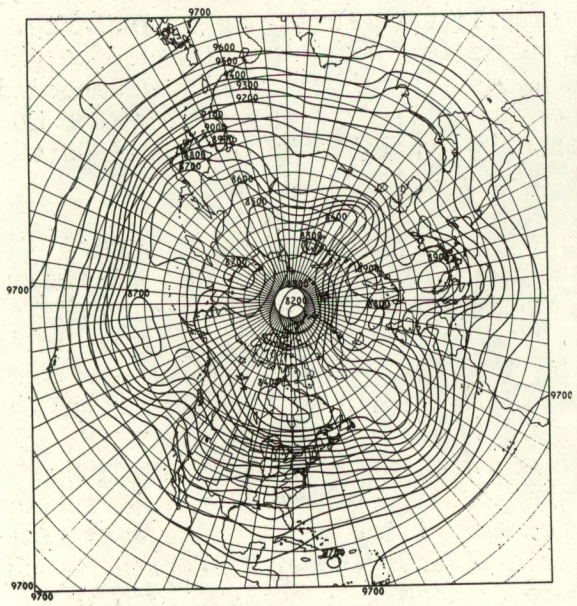

c. Final analysis

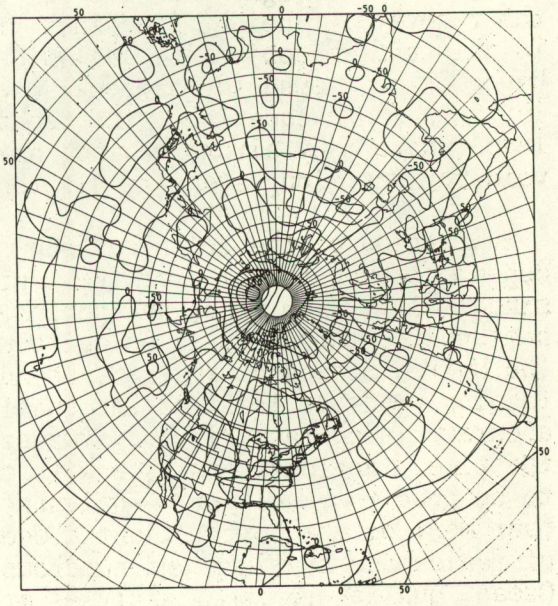

d. Final analysis minus the NMC analysis

Figure 9.--CRAM analyses and their comparisons with the NMC analysis for 18 January 1970, 0000 GMT. Nondivergent wind case.

The divergent version of the final analysis for this date is given in figure 8c. This map very closely resembles the NMC analysis. The difference field for the final analysis, shown in figure 8d, compared with that for the balanced height analysis has markedly lower values, generally in the range $\pm$ 50 meters. One region of large difference values occurs near the North Pole where no observations of any kind are available. The remaining pattern of difference values is seen to be correlated with ridges and troughs as in the balanced height analysis, but the amplitudes are much lower. Figures 9c and 9d illustrate final analysis maps for the nondivergent wind case and are seen to be essentially identical to their counterparts in figures 8c and 8d. From these results we may conclude that the divergent property of the wind field is important only in very large interpolation regions; for smaller interpolation regions normally found in the final analysis it is negligible.

Of most importance here is the finding that the final CRAM analysis and the NMC analysis are virtually equivalent. No claim of superiority can be made for either technique. However, this study has made it possible to evaluate the accuracy of the final CRAM analysis and, equivalently the NMC analysis, in regions of interpolated heights influenced by wind reports. From the results of section 3.3, we may state that most of the time (80 to 85%) either analysis technique will provide reliable reference level height values in these interpolation regions.

4.0 SUMMARY AND CONCLUSIONS

An accurate height analysis is required to provide a reference level for the recovery of height soundings from satellite measurements of radiance. To this end, an objective analysis technique for analyzing pressure height has been developed to make full use of winds through the wind law embodied in the balance equation. The technique was applied to data at the 300-mb level where many aircraft winds are normally available in otherwise data void regions along standard air routes over the oceans.

Evaluation of the technique shows that the analysis accuracy is very dependent upon the size of the region within which height values are determined solely from winds and peripheral observations of height. Over a hemisphere, the analysis is quite unacceptable. For regions the size of the United States or smaller, bounded by some height observations and containing winds at least of the quality of edited aircraft winds, the analysis accuracy is characterized by rms errors of 30 meters or less about 85% of the time. Regional analyses with these error characteristics are judged to be good to excellent. Analyses of this quality generally may be achieved over most of the North Atlantic Ocean because of the relatively dense network of radiosonde stations and numerous aircraft winds. Over the North Pacific Ocean, quality regional analyses are more difficult to achieve because of the sparse network of radiosonde stations and the distribution of aircraft winds with respect to those stations. In particular, there is a large region in the mid-Pacific south of Alaska of questionable quality because of the general lack of wind and height observations.

Further evaluation shows that the best analyses using the balance equation and all available winds and radiosonde data are essentially identical to the

operational NMC analysis. It is impossible to state which type of analysis is superior. This study, however, has provided new estimates of the expected error of regional analyses.

It is concluded that the 300-mb height analysis, with the exceptions noted above, would provide a reliable reference level specification for the retrieval of satellite-derived vertical height profiles.

ACKNOWLEDGMENTS

Special appreciation is extended to Dr. Christopher Hayden of the Meteorological Satellite Laboratory for his thorough and enlightening review of the manuscript and for his many useful suggestions offered throughout the course of this study.

Mr. Fred Nagle, also of this laboratory, freely gave his time and talents to help apply his personally developed computer programs for producing graphical displays of the analyses.

REFERENCES

Arnason, G., Haltiner, G.T. and Frawley, M.J., 1962: Higher-order Geostrophic Wind Approximations. Monthly Weather Review, 90, 175-185.

Deutscher Wetterdienst, 1960: Part F, "Transformation of the Basic Equations of Dynamic Meteorology into Coordinates of Stereographic Projection for the Purpose of Numerical Weather Prediction." Research in Objective Weather Forecasting, Final Report, Contract AF 61 (514)-1211 with Air Force Cambridge Research Center; Research Division, Deutscher Wetterdienst, Offenbach/M-Germany, 23 pp.

Endlich, R.M., 1967: An Iterative method for Altering the Kinematic Properties of Wind Fields. Journal of Applied Meteorology, 6, 837-844.

Endlich, R.M., Mancuso, R.L. and Shigeishi, H., 1971: Computation of Upper Tropospheric Reference Heights for Applying SIRS Data in Objective Analysis. Final Report, Contract 0-35199, Stanford Research Institute, Menlo Park, California, 73 pp.

Haltiner, G.J., and Martin, F.L., 1957: Dynamical and Physical Meteorology. McGraw-Hill Book Co., New York

Mancuso, R.L., 1967: A Numerical Procedure for Computing Fields of Stream Function and Velocity Potential. Journal of Applied Meteorology, 6, 994-1001.

Nagle, R.E., and Hayden, C.M., 1971: The Use of Satellite-Observed Cloud Patterns in Northern-Hemisphere 500-mb Numerical Analysis. NOAA Technical Report, NESS 55, 37 pp.

Phillips, N.A., 1959: On the Problem of Initial Data for the Primitive Equations. Tellus, 12, 121-126.

Rosenthal, S.L. 1960: Concerning the Feasibility of Computing the Field of Pressure-Geopotential from Observed Winds by Use of the Divergence Equation. Technical Report, No. 15, Contract NONR-1600(00), Florida State University, Department of Meteorology, 25 pp.

Smith, W.L., Woolf, H.M. and Fleming, H.E., 1972: Retrieval of Atmospheric Temperature Profiles from Satellite Measurements for Dynamical Forecasting. Journal of Applied Meteorology, 11, 113-122.

Stackpole, J.D., 1969: Operational Prediction Models at the National Meteorological Center. ESSA, U. S. Department of Commerce.

Thomasell, A., and Welsh, J.G., 1963: Studies of Techniques for the Analysis and Prediction of Temperature in the Ocean. Part 1, The Objective Analysis of Sea Surface Temperature. Technical Report 7046-70, The Travelers Research Center, Hartford, Connecticut. 52 pp.

Thomasell, A., Harris, R.G. and Welsh, J.G., 1966: Studies of Techniques for the Analysis and Prediction of Temperature in the Ocean, Part III, Automated Analysis and Prediction. Tech. Report 7421-213, The Travelers Research Center, Hartford, Connecticut, 97 pp.

Thomasell, A. and Welsh, J.G., 1968: Studies of Techniques for the Analysis and Prediction of Temperature in the Ocean, Part VI, Translation of Asynoptic Data. Tech. Report 7487-306, The Travelers Research Center, Hartford, Connecticut, 51 pp.

*U.S. GOVERNMENT PRINTING OFFICE:1976 210-801/176 1-3

(Continued from inside front cover)

NESC 53 Archiving and Climatological Applications of Meteorological Satellite Data. John A. Leese, Arthur L. Booth, and Frederick A. Godshall, July 1970, pp. 1-1--5-8 plus references and appendixes A through D. (COM-71-00076)

NESC 54 Estimating Cloud Amount and Height From Satellite Infrared Radiation Data. P. Krishna Rao, July 1970, 11 pp. (PB-194-685)

NESC 56 Time-Longitude Sections of Tropical Cloudiness (December 1966-November 1967). J. M. Wallace, July 1970, 37 pp. (COM-71-00131)

NOAA Technical Reports

NESS 55 The Use of Satellite-Observed Cloud Patterns in Northern Hemisphere 500-mb Numerical Analysis. Roland E. Nagle and Christopher M. Hayden, April 1971, 25 pp. plus appendixes A, B, and C. (COM-73-50262)

NESS 57 Table of Scattering Function of Infrared Radiation for Water Clouds. Giichi Yamamoto, Masayuki Tanaka, and Shoji Asano, April 1971, 8 pp. plus tables. (COM-71-50312)

NESS 58 The Airborne ITPR Brassboard Experiment. W. L. Smith, D. T. Hilleary, E. C. Baldwin, W. Jacob, H. Jacobowitz, G. Nelson, S. Soules, and D. Q. Wark, March 1972, 74 pp. (COM-72-10557)

NESS 59 Temperature Sounding From Satellites. S. Fritz, D. Q. Wark, H. E. Fleming, W. L. Smith, H. Jacobowitz, D. T. Hilleary, and J. C. Alishouse, July 1972, 49 pp. (COM-72-50963)

NESS 60 Satellite Measurements of Aerosol Backscattered Radiation From the Nimbus F Earth Radiation Budget Experiment. H. Jacobowitz, W. L. Smith, and A. J. Drummond, August 1972, 9 pp. (COM-72-51031)

NESS 61 The Measurement of Atmospheric Transmittance From Sun and Sky With an Infrared Vertical Sounder. W. L. Smith and H. B. Howell, September 1972, 16 pp. (COM-73-50020)

NESS 62 Proposed Calibration Target for the Visible Channel of a Satellite Radiometer. K. L. Coulson and H. Jacobowitz, October 1972, 27 pp. (COM-73-10143)

NESS 63 Verification of Operational SIRS B Temperature Retrievals. Harold J. Brodrick and Christopher M. Hayden, December 1972, 26 pp. (COM-73-50279)

NESS 64 Radiometric Techniques for Observing the Atmosphere From Aircraft. William L. Smith and Warren J. Jacob, January 1973, 12 pp. (COM-73-50376)

NESS 65 Satellite Infrared Soundings From NOAA Spacecraft. L. M. McMillin, D. Q. Wark, J.M. Siomkajlo, P. G. Abel, A. Werbowetzki, L. A. Lauritson, J. A. Pritchard, D. S. Crosby, H. M. Woolf, R. C. Luebbe, M. P. Weinreb, H. E. Fleming, F. E. Bittner, and C. M. Hayden, September 1973, 112 pp. (COM-73-50936/6AS)

NESS 66 Effects of Aerosols on the Determination of the Temperature of the Earth's Surface From Radiance Measurements at 11.2 μm. H. Jacobowitz and K. L. Coulson, September 1973, 18 pp. (COM-74-50013)

NESS 67 Vertical Resolution of Temperature Profiles for High Resolution Infrared Radiation Sounder (HIRS). Y. M. Chen, H. M. Woolf, and W. L. Smith, January 1974, 14 pp. (COM-74-50230)

NESS 68 Dependence of Antenna Temperature on the Polarization of Emitted Radiation for a Scanning Microwave Radiometer. Norman C. Grody, January 1974, 11 pp. (COM-74-50431/AS)

NESS 69 An Evaluation of May 1971 Satellite-Derived Sea Surface Temperatures for the Southern Hemisphere. P. Krishna Rao, April 1974, 13 pp. (COM-74-50643/AS)

NESS 70 Compatibility of Low-Cloud Vectors and Rawins for Synoptic Scale Analysis. L. F. Hubert and L. F. Whitney, Jr., October 1974, 26 pp. (COM-75-50065/AS)

NESS 71 An Intercomparison of Meteorological Parameters Derived From Radiosonde and Satellite Vertical Temperature Cross Sections. W. L. Smith and H. M. Woolf, November 1974, 13 pp. (COM-75-10432/AS)

NESS 72 An Intercomparison of Radiosonde and Satellite-Derived Cross Sections During the AMTEX. W. C. Shen, W. L. Smith, and H. M. Woolf, February 1975, 18 pp. (COM-75-10439/AS)